Phytomedicine 97 (2022) 153923

Contents lists available at ScienceDirect

Phytomedicine

journal homepage: www.elsevier.com/locate/phymed

Original Article

Granatin B and punicalagin from Chinese herbal medicine pomegranate peels elicit reactive oxygen species-mediated apoptosis and cell cycle arrest in colorectal cancer cells

Xiao-Xin Chen [a,b,*], Sheamin Khyeam [b], Zhang-Jin Zhang [a], Kalin Yan-Bo Zhang [a,*]

[a] School of Chinese Medicine, LKS Faculty of Medicine, University of Hong Kong, Sassoon Road, Pokfulam, Hong Kong
[b] Cardiovascular Research Institute & Department of Physiology, University of California, San Francisco, CA, USA

ARTICLE INFO

Keywords:
Colorectal cancer
Mucositis
Granatin B
Punicalagin
Pomegranate peel
Reactive oxygen species

ABSTRACT

Background: Colorectal cancer ranks among the most common cancers. 5-Fluorouracil (5-FU) based first-line chemotherapy for colorectal cancer treatment often leads to chemoresistance and gastrointestinal mucositis.
Purpose: This study aimed to find potential therapeutic agents from herbal medicine with anti-colorectal cancer and anti-mucositis activities.
Methods: Chinese medicine theory, network pharmacology analyses, and antioxidant activity coupled with liquid chromatography tandem mass spectrometry analyses were used to identify potential bioactive compounds. HT-29 human colorectal cancer cell culture and xenograft tumor models were employed to study anti-colorectal cancer efficacy. Lipopolysaccharide-induced RAW 264.7 and 5-FU treated Dark Agouti rats were used to evaluate anti-inflammatory and anti-mucositis activities. Histological staining, immunofluorescence imaging, western blots, and flow cytometric analyses were employed to explore the underlying mechanisms.
Results: Both Chinese medicine theory and network pharmacology analyses indicated pomegranate peels as a potential anti-colorectal cancer and anti-mucositis agent. Antioxidant activity coupled with liquid chromatography tandem mass spectrometry analyses revealed granatin B and punicalagin as the most potent antioxidant compounds in pomegranate peels. Granatin B and punicalagin demonstrated superior anti-colorectal cancer activities in both cell culture and xenograft tumor models. Granatin B and punicalagin also exhibited strong anti-inflammatory activities in lipopolysaccharide-induced RAW264.7 cells and anti-mucositis activities in 5-FU-treated rats. Mechanistic studies revealed that granatin B and punicalagin induced reactive oxygen species-mediated S-phase cell cycle arrest and apoptosis in HT-29 cells. Moreover, these compounds sensitized HT-29 cells to 5-FU-induced cell death and S-phase cell cycle arrest.
Conclusion: We report that granatin B and punicalagin exhibit superior anti-colorectal cancer and anti-mucositis activities. To the best of our knowledge, these results are novel and suggest that utilizing phenols from herbal medicine, such as granatin B and punicalagin, to target reactive oxygen species may be an innovative therapy to treat colorectal cancer and intestinal mucositis.

; ABTS, 2,2′-azino-bis(3-ethylbenzothiazoline-6-sulfonic acid) diammonium salt; DAF-FM, diaminofluorescein-FM; DCF-DA, 2',7'-dichlorofluorescin diacetate; DMEM, Dulbecco's Modified Eagle Medium; DMSO, dimethyl sulfoxide; DPPH, 2,2-diphenyl-1-picrylhydrazyl; FBS, fetal bovine serum; 5-FU, 5-fluorouracil; GAE/g d.w., gallic acid equivalent/g dry weight; HPLC-DAD-ESI-MS/MS, high performance liquid chromatography-diode array detector coupled with electrospray ionization tandem mass spectrometry; IC50, 50 % activity inhibition dose; JC-1, tetraethylbenzimidazolylcarbocyanine iodide; ROS, reactive oxygen species; NAC, N-acetyl-L-cysteine; MMP, mitochondrial membrane potential; MTT, 3-(4,5-dimethylthiazol-2-yl)-2,5-diphenyltetrazolium bromide; PBS, phosphate buffer solution; PI, propidium iodide; RPMI, Roswell Park Memorial Institute; SOD, superoxide dismutase; TCMID, Traditional Chinese Medicines Integrated Database; TCMSP, Traditional Chinese Medicine Systems Pharmacology.

* Corresponding authors at: School of Chinese Medicine, LKS Faculty of Medicine, University of Hong Kong, Sassoon Road, Pokfulam, Hong Kong.
E-mail addresses: xiaoxin.chen@ucsf.edu (X.-X. Chen), ybzhang@hku.hk (K.Y.-B. Zhang).

https://doi.org/10.1016/j.phymed.2022.153923
Received 1 October 2021; Received in revised form 18 December 2021; Accepted 2 January 2022
Available online 4 January 2022

Introduction

Colorectal cancer ranks in the top five most common cancers and is the third leading cause of cancer-related deaths in the United States (Wild et al., 2020). In recent years, the development of new therapeutic methods has led to significant improvements in treatment outcomes. However, the heterogeneity of colorectal cancer renders current chemotherapies and targeted therapies less effective. Particularly, for patients in advanced stages of the disease, drug resistance and adverse effects, especially mucositis, remain to be resolved (Zhang et al., 2017a). Therefore, novel approaches to overcome these setbacks are urgently needed.

Cancer is intricately related to apoptosis, a classical form of programmed cell death (Ouyang et al., 2012). Uncontrolled cell multiplication and inhibition of apoptosis are prerequisites for neoplastic evolution to occur. The rapid replication of cancer cells makes them more vulnerable to oxidative stress in the tumor microenvironment. Therefore, chemotherapies may be selectively toxic to cancer cells because they further augment oxidant stress and push these already stressed cells beyond their limits (Schumacker, 2006). Polyphenols can become pro-oxidants to generate this additional oxidative stress in cancer cells, primarily through the generation of reactive oxygen species (ROS) (Khan et al., 2014). We have previously reported that polyphenols from Chinese herbal medicine pomegranate peels induce apoptosis in colorectal cancer cells (Chen et al., 2018).

In this study, we further characterize the anti-cancer benefits of pomegranate peels. First, we screened various Chinese herbal medicine with anti-colorectal cancer and anti-mucositis activities in China Pharmacopeia using traditional Chinese medicine theory and network pharmacology. Pomegranate peels were identified as a potential source for anti-colorectal cancer and anti-mucositis therapeutic agents. Among pomegranate peel components, granatin B and punicalagin were revealed as potent antioxidants. We explored these antioxidants' anti-colorectal cancer and anti-mucositis activities and further investigated underlying mechanisms. The results of our study indicate that Chinese medicine theory and network pharmacology can be very powerful tools to reveal the molecular mechanisms of Chinese herbal medicine and support the development and standardization of Chinese herbal medicine as a potential therapeutic.

Materials and methods

Chemicals and reagents

Ellagic acid (EA), gallic acid (GA), ascorbic acid, 2,2-diphenyl-1-picrylhydrazyl (DPPH), 2′-azino-bis(3-ethylbenzothiazoline-6-sulfonic acid) diammonium (ABTS), Sephadex LH-20, 3-(4,5-dimethylthiazol-2-yl)-2,5-diphenyltetrazolium bromide (MTT), Hoechst 33,342, propidium iodide (PI), tetraethylbenzimidazolylcarbocyanine iodide (JC-1), 2′,7′-dichlorofluorescin diacetate (DCF-DA), acridine orange (AO), diaminofluorescein-FM (DAF-FM), and lipopolysaccharides (LPS) were from Sigma-Aldrich (St. Louis, MO, USA). Acetone, ethyl acetate, acetic acid, and acetonitrile (ACN) were provided by Duksan Pure Chemicals (Ansan, Korea). Fetal bovine serum (FBS), Roswell Park Memorial Institute (RPMI) medium, Dulbecco's Modified Eagle Medium (DMEM), penicillin-streptomycin, 0.25% trypsin-EDTA, and RNase A were from Gibco (Life Technologies, Carlsbad USA). H2O was purified by Milli-Q Synthesis A10 Water Purification System (Bedford, MA, USA).

Traditional Chinese medicine theory and network pharmacology analyses

After searching China Pharmacopoeia 2010, 97 herbs of the large intestine meridian were identified, twenty-three of which are commonly used as intestinal cancer treatments (China Pharmacopoeia, 2010). Pomegranate peels, with warm, sour, and astringent properties and traditionally used to treat symptoms like those exhibited in colorectal cancer and mucositis, was selected for network pharmacology analysis.

Compounds in pomegranate peels were collected from the Traditional Chinese Medicine Integrated Database (TCMID), Traditional Chinese Medicine Systems Pharmacology (TCMSP) database, Traditional Chinese Medicine Database@Taiwan, and literature search (Fischer et al., 2011; Mohammad and Kashani, 2012; Poyrazoglu et al., 2002). Significantly related pathways and diseases of the compounds were revealed by enrichment analysis of the compound-protein interactions (JEPETTO) and compound-gene interactions (DAVID 6.8), respectively. The flowchart of this analysis is shown in Fig. 1A.

Preparation of pomegranate peel ellagitannins

Pomegranate peels were provided by Hong Kong Hospital Authority-certified Chinese Medicine suppliers (Hong Kong, China). For antioxidant activity-guided analysis, 25 mg of pomegranate peel powders was extracted three times with 1 ml of the solvents–20%, 40%, 60% and 80% of aqueous acetone, methanol, and ethanol–respectively. The extracts were combined and diluted to 10 ml with water for further analysis. Preparation procedures for the punicalagin fraction as well as punicalagin and granatin B fraction were previously described (Chen et al., 2018). From 20 g of pomegranate peel powder, 1.32 ± 0.14 g of punicalagin and 0.82 ± 0.25 g of the granatin B and punicalagin rich fraction were obtained, respectively. The punicalin rich fraction was extracted from 1 g of pomegranate peel powder with 20% aqueous methanol (3 × 40 ml) and yielded 388.9 ± 32.09 mg. Acid hydrolysis was carried out to degrade granatin B and punicalagin as described in our previous report (Oszmianski et al., 2007). The purity of punicalagin in terms of mass conversion yield to its hydrolyzed products was 53.32 ± 1.21% (gallic acid: 3.49 ± 0.37%; ellagic acid: 49.83 ± 1.15%) as determined by HPLC analysis using gallic acid and ellagic acid as standards (Fig. S1). The purity of the granatin B and punicalagin rich fraction was 62.83% ± 1.32% (gallic acid: 14.92 ± 0.46%; ellagic acid: 47.91 ± 2.08%).

Antioxidant activity and LC-MS/MS analyses

Total phenolics and ABTS free radical scavenging activity assays have been previously described (Chen et al., 2014, 2017a). DPPH•-HPLC and ABTS•$^{+}$-HPLC assays were performed as described (Zhang et al., 2017c).

LC-MS/MS analysis was performed by an Agilent 1290 infinity LC system with API 3200 Q Trap and controlled by Analyst software (Chen et al., 2018). Mobile phase A was 0.2% acetic acid aqueous solution and B was ACN. The elution profile was: 95% A, 0–10 min; 95−70% A, 10−50 min; 70−20% A, 50−55 min; 20−95% A, 55−60 min.

Animals and ethics statement

Dark Agouti (DA) rats (female, body weight: 100–140 g, age 6 weeks) and BALB/c nude mice (male/female, body weight: 14–16 g, age 6 weeks) were kept under a 12 h light/dark cycle at 20 ± 5 °C with a standard diet and free access to water. The experiment protocols were approved by the Committee on the Use of Live Animals in Teaching & Research of the University of Hong Kong, protocol numbers: 4147–16 (approval date: December 14, 2016) and 4021–16 (approval date: June 16, 2016). Results were reported according to ARRIVE guidance (Kilkenny et al., 2010).

Mucositis model and treatments

A DA rat model of 5-FU-induced mucositis was employed as described (Chen et al., 2017a). Before treatment, the animals were acclimatized to the environment for 3 days. To determine the effects of the three ellagitannin fractions, the animals were treated with each of the fractions by oral gavage once per day at 100 mg/kg body weight for one week before induction of mucositis with a single intraperitoneal

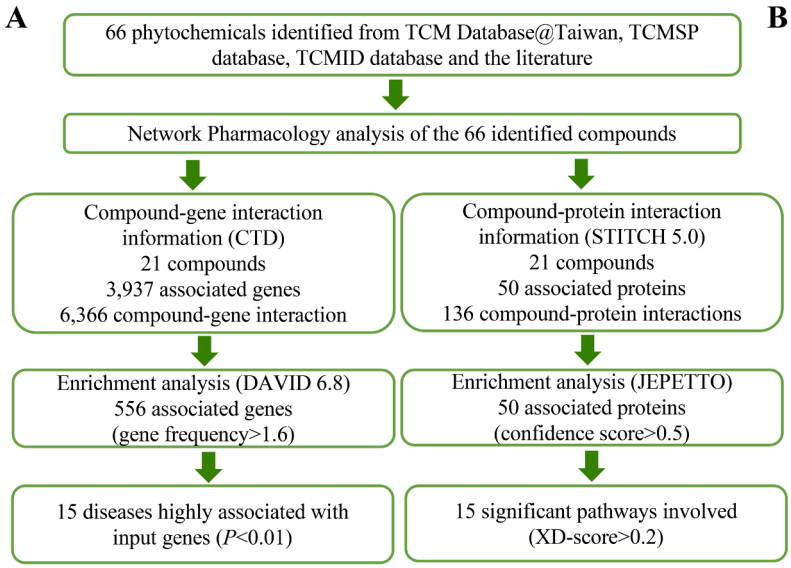

B

Disease Class	Number of input genes involved in the disease	*P* value
Cancer	315	5.1E-81
Immune	233	1.6E-34
Infection	178	2.1E-27

Pathway	XD-score	q value
Colorectal cancer	0.34924	0.00022
VEGF signaling pathway	0.27912	0.00137
mTOR signaling pathway	0.21676	0.01546
Toll-like receptor signaling pathway	0.20134	0.00137

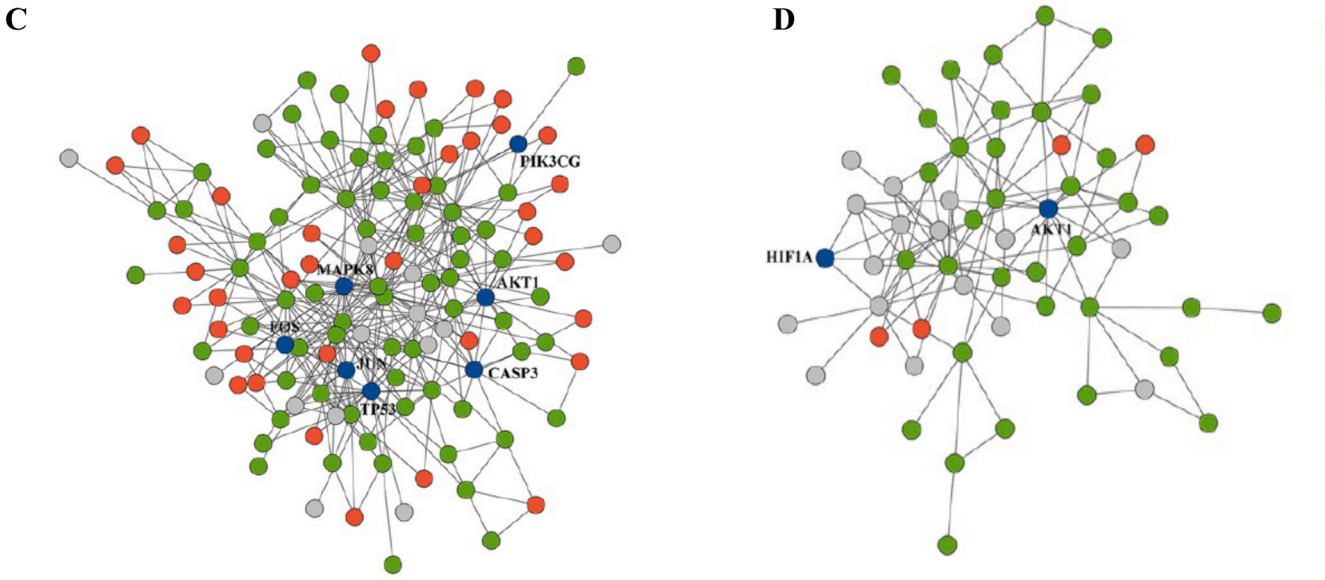

Fig. 1. Network pharmacology analysis of pomegranate peel compounds. **(A)** Flowchart for network pharmacology analysis. (**B**) Examples of significantly enriched pathways or disease class. (**C,D**) Colorectal cancer and toll-like receptor network. Gray circles indicate proteins in the target set, green circles indicate proteins of significantly related pathways, blue circles represent the overlaps between the pathway related proteins and input target proteins (For interpretation of the references to color in this figure legend, the reader is referred to the web version of this article.).

injection of 5-FU at 150 mg/kg body weight. Treatments continued for 2 more days before harvest on the third day.

Xenograft model and drug treatment

Mice acclimatized to the environment for 7 days. Then, HT-29 cells (1×10^6 cells in 100 μl of PBS) were injected into the right flank of nude mice via subcutaneous injection. Five days post injection, the mice were randomly separated into control and treatment groups (100 mg/kg body weight). The dose used was based on the maximum dose testing data (Fig. S2). Mice in the control and treatment groups were respectively gavaged with water or samples in water once every day for 28 days. Tumor volumes and body weights were measured twice per week. At the endpoint, the mice were euthanized by injection with an overdose of pentobarbitone. Tumors and organs were collected, weighed, and further analyzed.

Histological analysis

The proximal jejunum and organs were stained with hematoxylin and eosin and analyses of micrograph were done blindly as previously described (Chen et al., 2018).

Cell culture and treatments

HT-29 and RAW 264.7 cells were from ATCC and cultured respectively in RPMI or DMEM medium supplemented with 10% FBS, 100 units/ml penicillin, and 100 μg/ml streptomycin. The cells were analyzed by multiplex PCR with Applied Biosystems AmpF/STR Identifier Kit and confirmed by the ATCC STR database. For experiments, the cells were seeded at 5.0×10^3 cells/well, 1.0×10^5 cells/well, and 5.0×10^5 cells/well in 96-well, 24-well, and 6-well culture plates, respectively. After 12–24 h incubation, the medium was replaced with medium containing test samples. The samples were dissolved in dimethyl sulfoxide (DMSO). DMSO-treated cells were used as a control.

Cell viability analysis

MTT assay was performed as described (Chen et al., 2017a). DMSO was used to dissolve the formazan crystals. Absorbance was read at 540 nm using a microplate reader (CLARIOstar, BMG Labtech, Germany).

Apoptosis analysis

Fluorescence microscopy of Hoechst 33,342 and PI double stained cells (imaged by Axiovert S-100 Zeiss fluorescence microscope, Carl Zeiss, Zürich, Switzerland) and flow cytometry of BD Pharmingen FITC Annexin V Apoptosis Detection Kit I (BD Biosciences, San Diego, USA) stained cells (acquired by FACS Canto II Analyzer, BD Biosciences) were used for apoptosis analysis. Experimental details have been previously described (Chen et al., 2017b; China Pharmacopea Committee, 2010).

Cell cycle analysis

PI staining was used. Data were acquired by the FACS Canto II Analyzer. Experimental details were as described (Chen et al., 2017b).

ROS and mitochondrial membrane potential (MMP) determination

ROS and MMP were determined by DCF-DA and JC-1 staining as described (Chen et al., 2018). Data were attained using the Zeiss fluorescence microscope or flow cytometer (FACS Canto II Analyzer).

Nitric oxide (NO) concentration determination

After treatments for 1 h, cells were incubated with 1 μg/ml of LPS for 24 h before No. concentrations were measured. Briefly, equal volumes of medium and Griess reagent (Sigma-Aldrich Chemical Co.) were mixed and incubated at room temperature in the dark for 10 min. The absorbance was read at 540 nm using the CLARIOstar microplate reader. Sodium nitrite was used as a standard.

Intracellular NO levels were determined using a DAF-FM fluorescence probe. Briefly, the cells were loaded with DAF-FM (5 μM) at 37 °C for 20 min and washed with PBS before imaging with the Zeiss fluorescence microscope.

AO staining

After treatments, 5 μg/ml of AO was added for 5 min. Cells were washed and fixed in 4% paraformaldehyde and washed again before imaging with the Zeiss fluorescence microscope.

Western blot

Experimental procedures and data analyses were previously described (Chen et al., 2017a). Cleaved caspase 3, caspase 8, LC 3, NF-κB p65, iNOS (rabbit, Cell Signaling Technology), p62, caspase 9 (mouse, Cell Signaling Technology), IL-6 (mouse, Abcam), and β-actin (mouse, Santa Cruz Biotechnology, Santa Cruz) primary antibodies, and horseradish peroxidase-conjugated secondary antibodies (goat, Cell Signaling Technology) were used.

Immunofluorescence staining

Experimental details were as described (Chen et al., 2018). NF-κB p65 primary antibody (rabbit, Cell Signaling Technology) and Alexa Fluor® 488 goat anti-rabbit IgG secondary antibody (Invitrogen) were used. The images were taken by LSM 700 confocal laser scanning microscope (Carl Zeiss, Jena, Germany).

Data analysis

Data were presented as mean±standard deviation and analyzed by GraphPad Prism 7.0 (San Diego, CA, USA) using unpaired *t*-test or one-way ANOVA with Tukey's post hoc test. Statistical significance was considered if $p < 0.05$.

Results

Network pharmacology analysis

Sixty-six chemicals were found in pomegranate peels (Table S1). In the chemical-gene interaction network analysis, 21 out of the 66 chemicals had 6366 chemical-gene interactions with 3937 related genes in the Comparative Toxicogenomics Database (CTD). Genes with frequencies under the average (<1.60) were excluded to reduce redundancy. The remaining 556 genes were subjected to gene enrichment analysis using DAVID. After limiting annotation to Homo sapiens, 550 genes were identified. Of these genes, "GAD_DISEASE_CLASS" was used to annotate significantly related diseases. Once nonspecific diseases class were discarded, 15 highly associated disease classes including cancer, immune disorders, and infections were identified (Fig. 1A,B).

For chemical-protein interaction analysis, 130 interactions and 50 proteins with a confidence score of greater than 0.5 were used for enrichment analysis to obtain association scores (XD-scores) and q values (significance of overlap) of the pathways involved. The XD-score and q-value algorithms showed that the threshold XD-score was 0.2. Using this threshold, 15 significant pathways including vascular endothelial growth factor (VEGF) signaling, mTOR signaling, and toll-like receptor (TLR) signaling pathways were identified (Fig. 1A,B). The chemical-protein interactions and the related significant signaling pathways were shown in Table S2. Among these pathways, VEGF pathway is upregulated in many tumors including colorectal cancer (Ahluwalia et al., 2014). mTOR has been reported as an effective drug target showing promising anti-colorectal cancer activity (Wang et al., 2020). Moreover, TLR signaling is involved in the immune cell response to microbes in the intestinal tract mucosa (Price et al., 2018). Apoptosis cell death-related proteins CASP3 and TP53 are targets in the colorectal cancer network (Fig. 1C); AKT1 is the target protein of compounds in both the colorectal cancer and TLR networks (Fig. C and D). Altogether, these results suggest that pomegranate peel compounds might be a promising source for developing therapeutic agents for colorectal cancer.

Antioxidant activity-guided analysis

To thoroughly extract active compounds from pomegranate peels, various aqueous concentrations of acetone, methanol, and ethanol were employed. For all three solvents, 60% aqueous extracts achieved the highest total phenolics yield (Fig. 2A, upper panel). The 60% aqueous extracts also exhibited the strongest free radical scavenging activities (Fig. 2A, middle and lower panels). There were significant correlations between total phenolic contents and DPPH• scavenging activities ($r = 0.6155$, $p = 0.0331$), total phenolic contents and $ABTS^{\bullet+}$ scavenging activities ($r = 0.6495$, $p = 0.0223$), and DPPH• scavenging activities and $ABTS^{\bullet+}$ scavenging activities ($r = 0.6894$, $p = 0.0131$) (Fig. 2B). These results indicate that phenolics are the major antioxidant component of the extracts.

In general, antioxidant activities of bioactive compounds in a cell-free system are good indicators of their biological activities. To identify the major antioxidant compounds, extracts were subjected to HPLC-DAD-ESI-MS-MS analysis and nine peaks were identified. The mass fragmentation results of the compounds were similar to those reported previously (Garcia-Villalba et al., 2015). The nine peaks were identified as gallic acid, gallagyl-hexoside (punicalin), digalloly-hexoside, galloyl-HHDP-hexoside, bis-HHDP-hexoside (pedunculagin I),

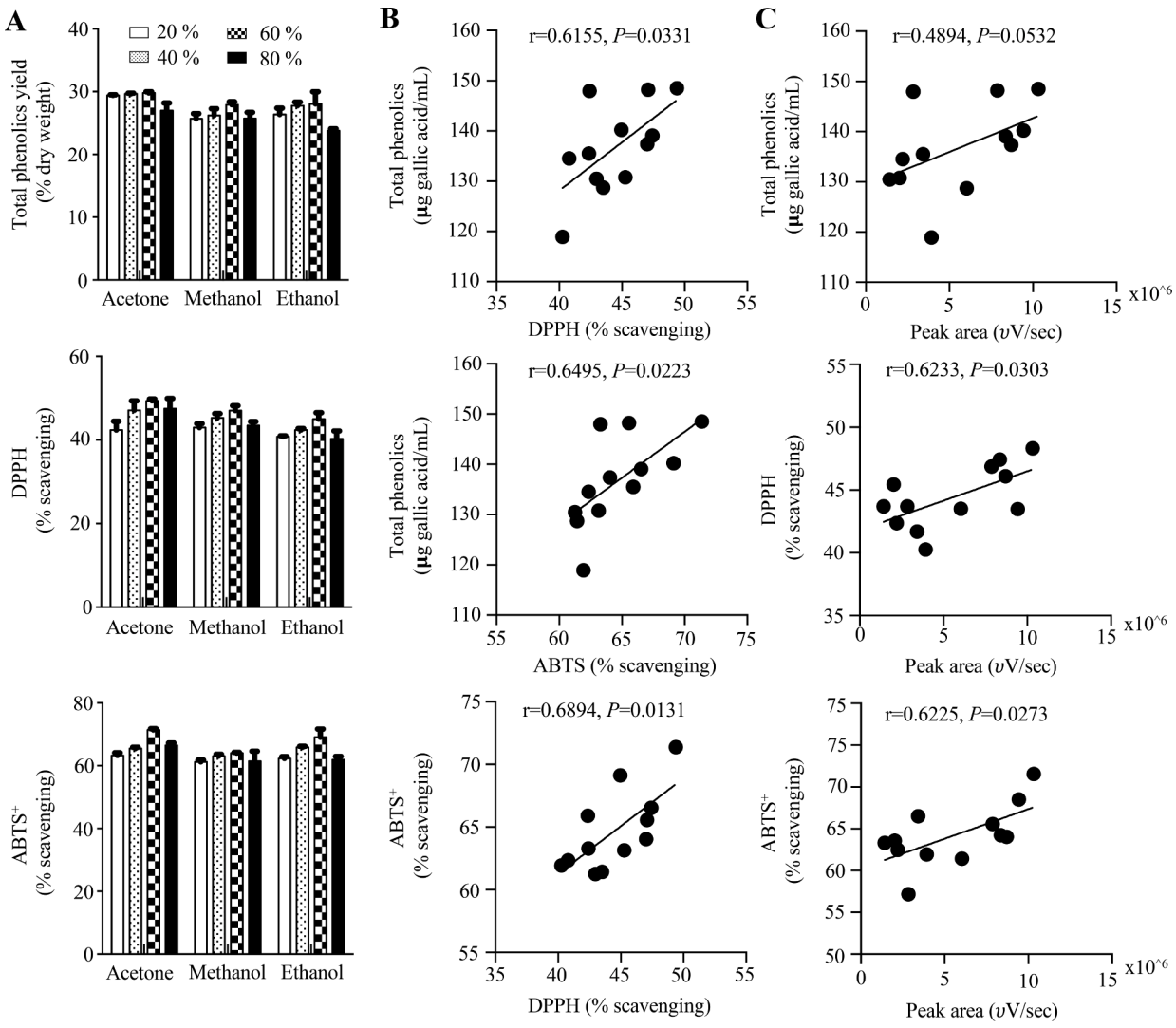

Fig. 2. Antioxidant activity-guided analyses. (**A**) Total phenolic contents and antioxidant activities of pomegranate peel extracts. The extracts were diluted 5 times before measurements. (**B**) Correlation among total phenolic contents, 2,2-diphenyl-1-picrylhydrazyl (DPPH) and 2,2′-azino-bis(3-ethylbenzothiazoline-6-sulfonic acid) diammonium ($ABTS^{+}$) free radical scavenging activities of pomegranate peel extracts. R represents Pearson's correlation coefficient. Strength of association, small: 0.1 to 0.3, medium: 0.3 to 0.5, large: 0.5 to 1.0. (**C**) Correlation of punicalagin peak areas with total phenolic contents as well as DPPH and ABTS free radical scavenging activities of pomegranate peel extracts. Values reported as mean ± SD. $n = 3$.

punicalagin-I, punicalagin-II, granatin B, and ellagic acid, respectively (Figs. S3, S4 and Table S3**)**. For the three solvents used, the highest yields of gallic acid, punicalin, digalloly-hexoside, galloyl-HHDP-hexoside, pedunculagin I were obtained with 20% or 40% aqueous solvents, while the highest yields of punicalagin-I and punicalagin-II were obtained using 60% aqueous solvents (Fig. S5). Moreover, there were strong correlations between total peak areas of punicalagin-I and punicalagin-II with total phenolics content ($r = 0.4894$, $p = 0.0532$), DPPH• scavenging activity ($r = 0.6233$, $p = 0.0303$), and $ABTS^{\bullet+}$ scavenging activity ($r = 0.6325$, $p = 0.0273$), indicating that punicalagin-I and punicalagin-II contribute to the potent free radical scavenging activities of the 60% aqueous extracts (Fig. 2C).

Pre-column reaction of samples with DPPH• followed by HPLC-DAD analysis is an efficient approach to identify the individual antioxidant compounds from complex samples by assessing decreasing peak areas (Sun et al., 2012). The 20% aqueous ethanol extracts had a chromatogram profile representative of pomegranate peel constituents and were thus analyzed first. Except for gallic acid and ellagic acid, all other compounds showed significantly decreased peak areas. These results were further confirmed by $ABTS^{\bullet+}$-HPLC-DAD analysis (Fig. S6). Then, samples with different major constituents were analyzed. For the punicalagin rich fraction, significantly decreased peak areas of punicalagin-I and punicalagin-II were observed (Fig. S6). In the granatin B and punicalagin rich fraction, punicalagin-II and granatin B peak areas were significantly decreased (Fig. S6). When hydrolyzed, the granatin B and punicalagin rich fraction showed a significantly decreased peak area of gallic acid, but not ellagic acid (Fig. S6). Collectively, these results indicate eight compounds, all except ellagic acid, directly react with DPPH• and $ABTS^{\bullet+}$.

To confirm that punicalagin-I, punicalagin-II, and granatin B were potent antioxidants, antioxidant activities of a crude punicalagin fraction, punicalagin rich fraction, and a granatin B and punicalagin rich fraction were examined. Total phenolic contents of the samples increased dose-dependently. Granatin B and punicalagin rich fraction had a higher phenolic content than the punicalagin rich fraction, which had a higher phenolic content compared to the crude punicalagin fraction (Fig. S7A**)**. Moreover, a dose-dependent $ABTS^{\bullet+}$ scavenging power was observed in the same order: granatin B and punicalagin rich fraction with the greatest, then the punicalagin rich fraction, and lastly the crude punicalagin fraction (Fig. S7B). The free radical scavenging activities of the punicalagin rich fraction as well as granatin B and punicalagin rich fraction were more potent than that of ascorbic acid (Fig. S7B). The IC_{50}

values of the punicalagin rich fraction, granatin B and punicalagin rich fraction, and ascorbic acid against ABTS$\bullet^{+}$ were 164.57 ± 11.53, 107.38 ± 3.17, and 395.66 ± 2.08 μg/ml, respectively. Therefore, these results not only suggest that both punicalagin and granatin B possess strong antioxidant activities but also indicate that granatin B exhibits stronger antioxidant activity than punicalagin.

In vitro and in vivo effects of granatin B and punicalagin on HT-29 cells

Using antioxidant activity as a proxy for anti-cancer activity, the fractions with potent antioxidant activities were selected for further studies in HT-29 human colorectal cancer cells. After treatment for 24 h at 80 μg/ml, the punicalagin rich fraction was not effective while the punicalin rich fraction reduced cell viability by 33.2 ± 4.4%, and the granatin B and punicalagin fraction achieved 60.1 ± 3.2% cell viability reduction. At 48 h, the 80 μg/ml punicalagin and punicalin rich fractions achieved 39.8 ± 4.6% and 46.7 ± 2.7% viability reduction, respectively, while the granatin B and punicalagin rich fraction was even more effective, achieving a 63.7 ± 0.75% viability reduction. At 72 h, all samples exhibited dose-dependent toxicity. Cell viability reductions at 80 μg/ml were 65.3 ± 2.4%, 86.2 ± 2.2%, and 61.9 ± 4.1% for the punicalin rich fraction, granatin B and punicalagin rich fraction, and punicalagin rich fraction, respectively (Fig. 3A).

Due to its effectiveness in reducing cell viability, the granatin B and

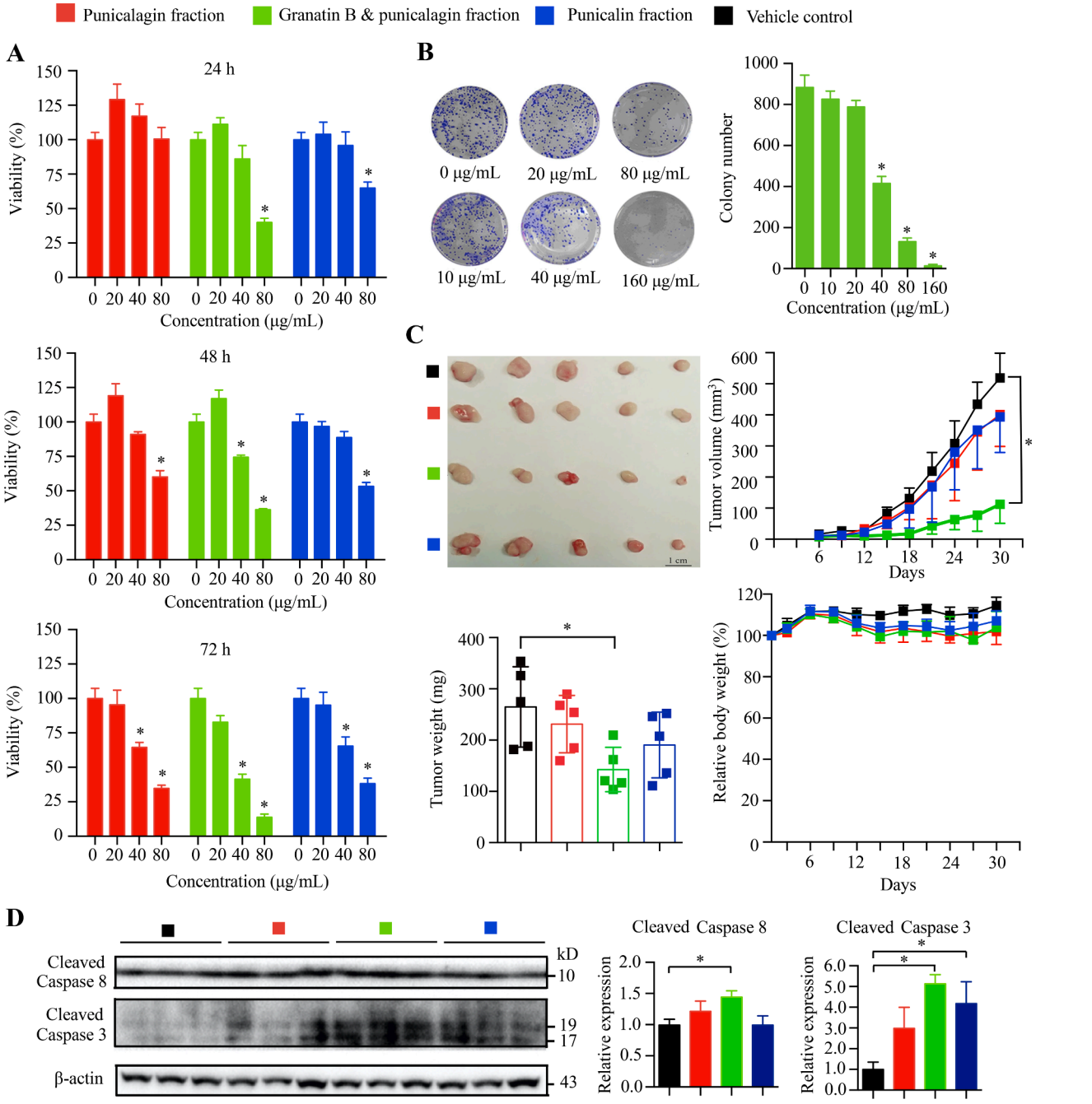

Fig. 3. Anti-HT-29 colorectal cancer activities of the ellagitannins. (**A**) Cell viability analysis. (**B**) Colony formation assay. Cells were incubated with granatin B and punicalagin fraction for 18 h and then allowed to grow for 2 weeks before analysis. (**C**) HT-29 tumor growth. Tumor images, tumor volume changes during the experiment, tumor weight, body weight changes during the experiment. (**D**) Western blot of the caspases in the xenograft tumors and quantitative results. Values reported as mean ± SD. A and B, $n = 3$. C and D, $n = 5$. Compared to control, $^{*}p < 0.05$.

punicalagin rich fraction was further tested. The granatin B and punicalagin rich fraction exhibited both time- and dose-dependent cytotoxicity (Fig. S8). The IC_{50} was 58.71 ± 4.57 μg/ml and 36.58 ± 4.24 μg/ml for 48 h and 72 h treatments, respectively. Furthermore, the colony formation assay showed a dose-dependent inhibition of colonies by the granatin B and punicalagin rich fraction (Fig. 3B). These results demonstrate that among the three fractions, the granatin B and punicalagin rich fraction exhibits the strongest toxicity towards HT-29 cells. Moreover, this further confirms the idea that the antioxidant activity of bioactive compounds in a cell-free system is a good indicator of their biological activities.

The *in vivo* effects of the fractions were then tested in a xenograft tumor model. Among the three samples, the granatin B and punicalagin rich fraction most effectively inhibited tumor growth without affecting body weight (Fig. 3C). Moreover, no obvious pathological changes in the major organs of mice were observed (Fig. S9). Granatin B and punicalagin induced apoptosis in the xenograft tumors as indicated by the increased cleavage of caspase 8 and caspase 3 (Fig. 3D). Original uncropped Western blot images are shown in Fig. S10. These results are consistent with the colorectal cancer network analysis indicating apoptotic cell death is involved.

Mechanism of granatin B and punicalagin-induced HT-29 cell death

Cell death mechanisms of the compounds were further explored *in vitro*. Hoechst 33,342 staining showed that cells treated with the three

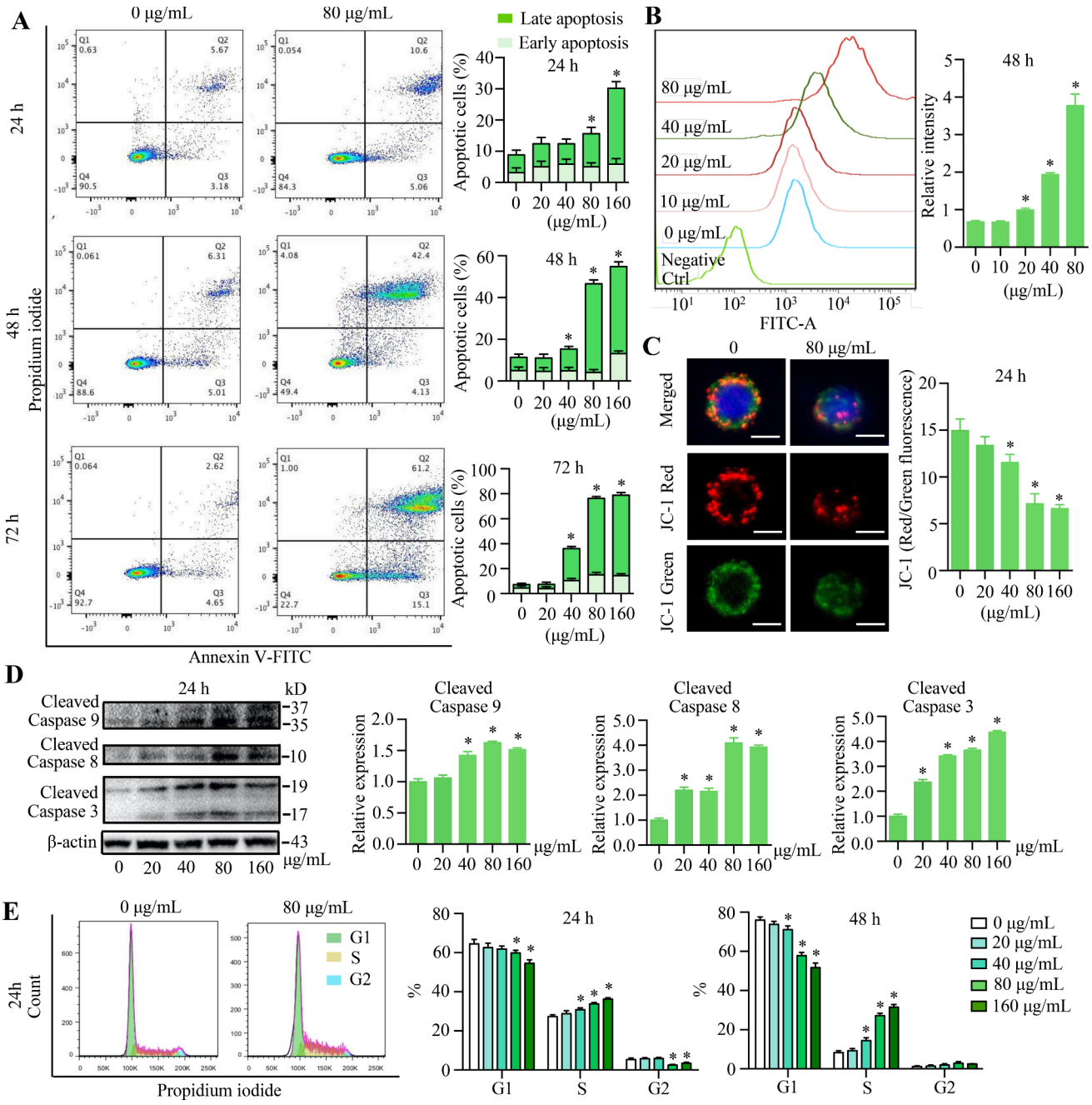

Fig. 4. Cell death mechanisms of granatin B and punicalagin against HT-29 colorectal cancer cells. (**A**) Representative flow cytometry of Annexin V-FITC/propidium iodide-stained cells and quantitative results. (**B**) Flow cytometry data of DCF-DA stained cells and quantitative results. (**C**) Fluorescent images of JC-1 stained cells 24 h after treatment. Scale bars: 10 μm. (**D**) Western blot of the caspases and quantitative results *in vitro*. (**E**) Cytometric analysis of the cell cycle. Histograms show representative cell cycle distribution patterns. Values reported as mean ± SD. A–F, $n = 3$. Compared to control, $^*p < 0.05$.

ellagitannin fractions at 40 μg/ml for 48 h exhibited typical characteristics of apoptosis such as chromatin condensation, karyopyknosis, and apoptotic body formation (Fig. S11A). Granatin B and punicalagin fraction-induced apoptosis was further analyzed with annexin V-FITC/PI double labeling. Increases in apoptosis were both dose- and time-dependent (Fig. 4A). At 24 h, there were 15.66 ± 1.62% and 30.21 ± 1.95% apoptotic cells in 80 μg/ml and 160 μg/ml treated groups, respectively, compared to 8.85 ± 1.53% in the control. At 48 h, apoptotic populations in 40 μg/ml, 80 μg/ml, and 160 μg/ml treatment groups reached 15.53 ± 1.45%, 46.35 ± 2.16%, and 54.80 ± 1.80%, respectively, compared to 11.32 ± 1.59% in the control. At 72 h, apoptotic cells in 40 μg/ml, 80 μg/ml, and 160 μg/ml treatment groups increased to 36.10 ± 1.75%, 76.30 ± 1.72%, and 79.00 ± 1.85%, respectively, compared to 7.18 ± 1.85% in the control. Collectively, these results indicate that apoptosis is the major mechanism of granatin B and punicalagin-induced HT-29 cell death.

To further explore the mechanism of apoptosis induced by granatin B and punicalagin, ROS and MMP in HT-29 cells were further evaluated. Treatment with the granatin B and punicalagin rich fraction for 48 h at 40 μg/ml increased ROS production more significantly than those treated with the punicalagin rich fraction or punicalin rich fraction (Fig. S11B). A dose-dependent increase of ROS production was observed after granatin B and punicalagin treatment at 48 h (Fig. 4B). Furthermore, JC-1 staining showed that a 40 μg/ml treatment of granatin B and punicalagin for 48 h could shift fluorescence from red to green more strikingly than punicalagin and punicalin, indicating a more dramatic decrease in MMP (Fig. S11C). A dose-dependent decrease of red to green fluorescence ratio was also observed after granatin B and punicalagin treatment for 24 h (Fig. 4C). These results indicate that granatin B and punicalagin might trigger ROS-mediated mitochondrial damage to induce apoptosis.

To further investigate the mechanisms underlying granatin B and punicalagin-induced apoptosis, cleavage of caspase family proteins was measured. Granatin B and punicalagin dose-dependently increased the levels of cleaved caspase 3, 8, and 9, indicating that both extrinsic and mitochondria-mediated apoptotic pathways are involved (Fig. 4D). Moreover, granatin B and punicalagin treatment decreased the protein levels of mitochondrial antioxidant protein superoxide dismutase 2 (SOD 2) without affecting cytoplasmic antioxidant protein SOD 1 expression (Fig. S12). Analyzing cell cycle activity, both 24 h and 48 h treatments dose-dependently arrested the cells in S-phase while reducing cells in G1-phase (Fig. 4E).

In summary, granatin B and punicalagin stimulate both extrinsic and intrinsic (mitochondria-mediated) apoptotic pathways. In the mitochondria-mediated apoptotic pathway, granatin B and punicalagin induce ROS stress in the mitochondria which further leads to the

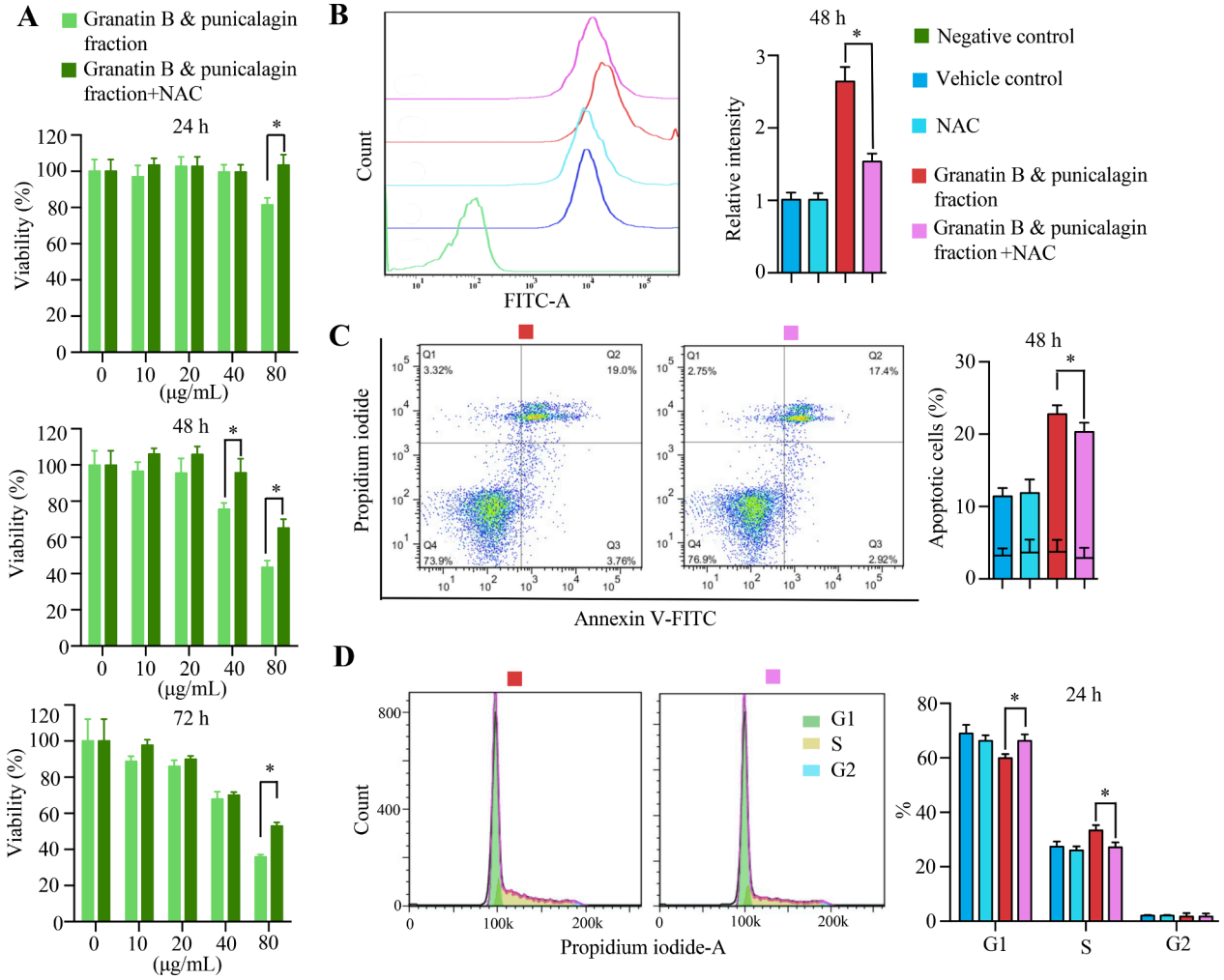

Fig. 5. Effects of antioxidants on granatin B and punicalagin-induced cell death in HT-29 colorectal cancer cells. (**A**) Cell viability analysis. Concentrations of granatin B and punicalagin fraction and N-acetyl cysteine (NAC) are 40 μg/ml and 3 mM, respectively. (**B**) Flow cytometry of DCF-DA-stained cells and quantitative results. Concentrations of granatin B and punicalagin fraction and NAC are 80 μg/ml and 3 mM, respectively. (**C**) Representative flow cytometry of Annexin V-FITC/propidium iodide-stained cells and quantitative results. (**D**) Representative flow cytometry of the cell cycle distribution and quantitative results. Concentrations of granatin B and punicalagin fraction and NAC are 80 μg/ml and 1 mM, respectively. Values reported as mean ± SD. *A* − *D*, $n = 3$. *$p < 0.05$.

decrease of MMP. Moreover, cell cycle arrest in S-phase also contributes to the toxicity of granatin B and punicalagin against HT-29 cells.

Effects of antioxidants on granatin B and punicalagin-induced HT-29 cell death

Antioxidant and ROS inhibitor, N-acetyl-l-cysteine (NAC) did not induce cytotoxicity in HT-29 cells at 3 mM (Fig. S13A). In fact, pre-treatment with 1 mM NAC significantly ameliorated the effect of granatin B and punicalagin on HT-29 cell viability at 24 h (Fig. S13B). Cell viability of 40 μg/ml and 80 μg/ml granatin B and punicalagin fraction-treated cells increased from 86.52 ± 7.77% and 57.50 ± 4.19% to 101.36 ± 8.51% and 86.10 ± 9.76%, respectively. At 48 h, only the viability of cells in the 80 μg/ml treatment group increased. Effects of higher concentrations of NAC on granatin B and punicalagin-induced cytotoxicity were further examined. Similarly, 3 mM NAC reduced the cytotoxic effects of granatin B and punicalagin (Fig. 5A). At 24 h, 3 mM NAC increased the viability of 80 μg/ml granatin B and punicalagin fraction-treated cells from 81.47 ± 3.94% to 103.42 ± 5.77%. At 48 h, 3 mM NAC increased the viability of 40 and 80 μg/ml granatin B and punicalagin fraction-treated cells from 75.51 ± 3.58% and 43.94% to 96.69 ± 7.77% and 65.22 ± 4.93%, respectively. At 72 h, only the viability of 80 μg/ml treated cells significantly increased. Altogether, these results indicate that antioxidants such as NAC can attenuate the cytotoxic effects granatin B and punicalagin have on HT-29 cells.

The mechanisms of how NAC ameliorated the effects of granatin B and punicalagin were further explored. NAC reduced granatin B and punicalagin-induced ROS (Fig. 5B) and apoptosis (Fig. 5C). Granatin B and punicalagin also significantly increased the cell population in S-phase, which was rescued by NAC. Simultaneously, the resulting decrease of G1-phase cells was also alleviated by NAC treatment (Fig. 5D). Collectively, these results indicate that granatin B and punicalagin-induced HT-29 cell apoptosis is due to, at least partially, ROS-mediated cell cycle arrest.

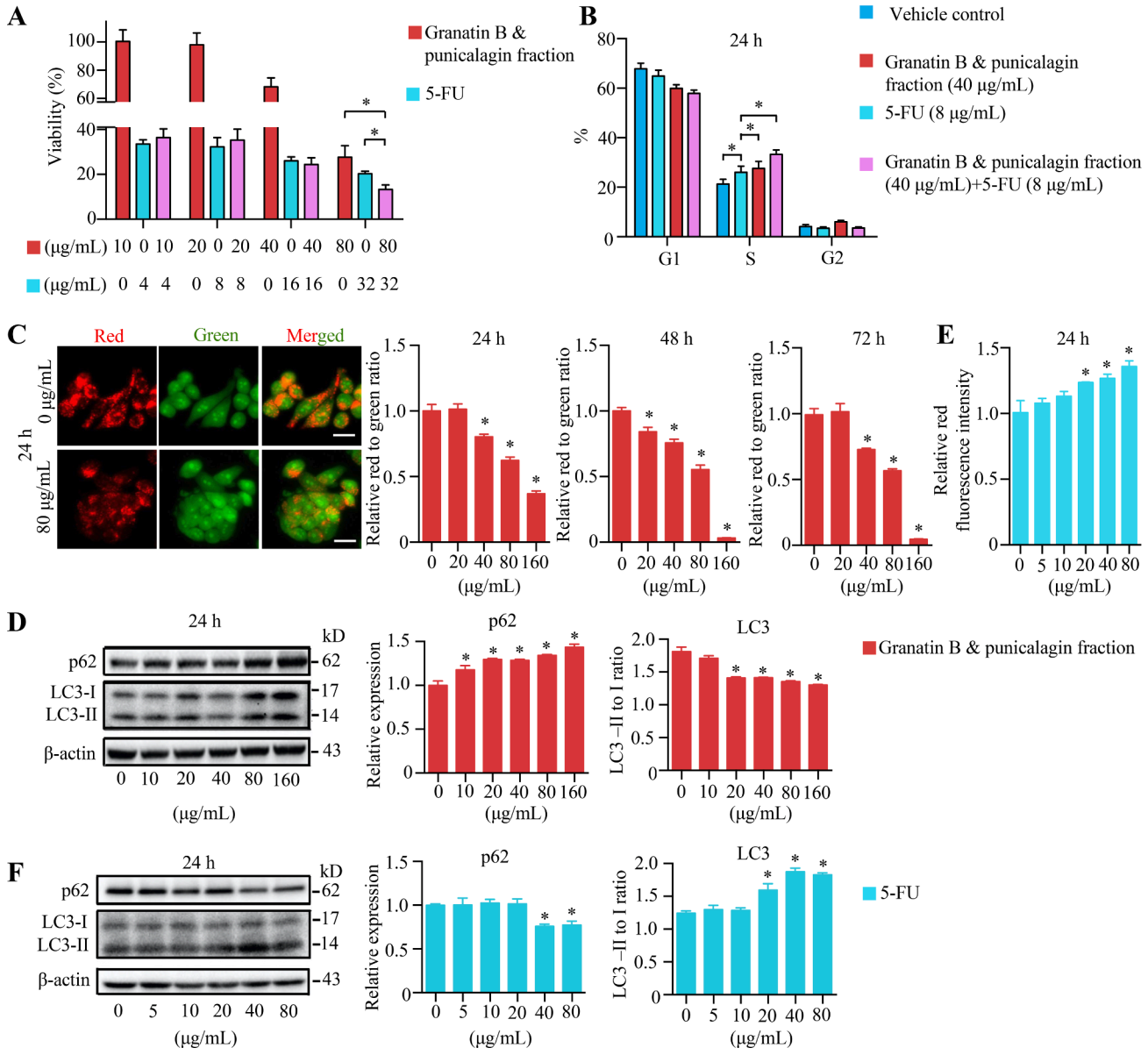

Fig. 6. Combined effects of granatin B and punicalagin with 5-FU on HT-29 colorectal cancer cells. (A) Cell viability. (**B**) Cell cycle distribution. (**C**) Representative images of acridine orange-stained cells treated with granatin B and punicalagin and quantitative results. Scale bars: 20 μm. (**D**) Western blot of LC3 and p62 and quantitative results after treatment with granatin B and punicalagin. (**E**) Quantitative results of acridine orange-stained cells treated with 5-FU. (**F**) Western blot of LC3 and p62 and quantitative results after treatment with 5-FU. Values reported as mean ± SD, $n = 3$. Compared to control, $^*p < 0.05$.

Effects of combined granatin B, punicalagin, and 5-FU treatment on HT-29 cells

Granatin B and punicalagin (80 μg/ml) significantly enhanced the cytotoxicity of 5-FU (32 μg/ml), an authorized chemotherapy medication used to treat colorectal cancers (Fig. 6A). At 24 h, treatment with 40 μg/ml of granatin B and punicalagin or 8 μg/ml of 5-FU significantly arrested cells in S-phase; combined treatment increased this cell population even further (Fig. 6B).

Autophagy is one mechanism leading to colorectal cancer cell resistance to 5-FU (Sui et al., 2014). Granatin B and punicalagin instead inhibits autophagy as suggested by the decrease of LC3 II/LC3 I, increase of p62 levels, and decrease of acidic vacuoles (Figs. 6C,D and S14). We also confirmed that 5-FU does induce autophagy in HT-29 cells as revealed by the increase of LC3 II/LC3 I, reduction of p62 levels, and increase of acidic vacuoles (Figs. 6E,F and S15). Furthermore, the inhibition of NF-κB p65 nuclear translocation has been shown to suppress cell proliferation and cell cycle activity, while inducing apoptosis (Zhang et al., 2017c). Thus, the effects of 5-FU in conjunction with granatin B and punicalagin on NF-κB p65 nuclear translocation were examined by immunofluorescence staining. Cells were treated with 80 μg/ml of granatin B, punicalagin, and 5-FU for 24 h. Granatin B and punicalagin treatment prevented p65 nuclear translocation, while 5-FU increased p65 nuclear import (Fig. S16). Collectively, these results

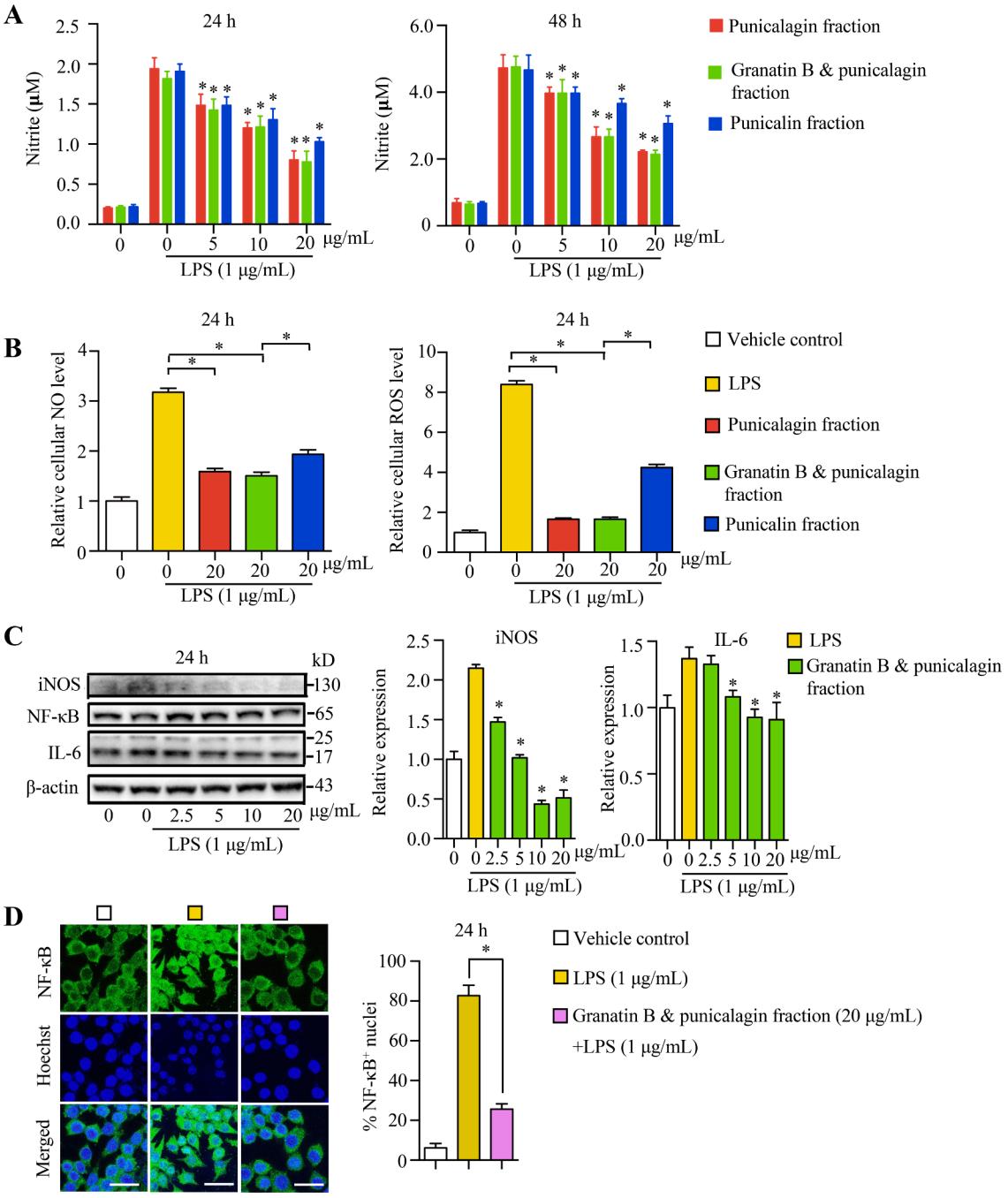

Fig. 7. Anti-inflammatory activities of the ellagitannins in LPS induced RAW 264.7 cells. (**A**) Griess test. (**B**) Quantitative DAF-FM and DCF-DA staining results. (**C**) Western blot of IL-6, iNOS, p65 and quantitative results. (**D**) Immunofluorescent staining of NF-κB p65. Histogram on the right shows quantitative results. More than 200 cells counted for each treatment. Scale bars: 20 μm. Values reported as mean ± SD, $n = 3$. Compared to LPS treatment group, $^{*}p < 0.05$.

demonstrate that granatin B and punicalagin might enhance the cytotoxicity of 5-FU against HT-29 cells by increasing cell cycle arrest and NF-κB signaling, while inhibiting autophagy.

Effects of granatin B and punicalagin on LPS-induced inflammation in RAW 264.7 cells

The ellagitannins were non-cytotoxic up to 20 μg/ml for both 24 h and 48 h treatments (Fig. S17). Cells were pretreated with nontoxic concentrations of the ellagitannins for 1 h and then stimulated with LPS for 24 h or 48 h. NO levels in the culture supernatants were determined by Griess test. The ellagitannins significantly inhibited LPS-stimulated NO secretion in RAW 264.7 cells dose-dependently, with granatin B and punicalagin showing the greatest inhibition and punicalin the least (Fig. 7A). NO cellular production was further measured by DAF-FM fluorescence staining. The ellagitannins (20 μg/ml) significantly decreased LPS-induced intracellular NO production (Fig. 7B). Consistent with the Griess test results, granatin B and punicalagin reduced cellular NO levels the most, followed by punicalagin, and finally punicalin.

Next, inhibitory effects of the ellagitannins on LPS-stimulated ROS generation in RAW 264.7 cells were further explored. The ellagitannins (20 μg/ml) significantly decreased LPS-induced ROS accumulation in

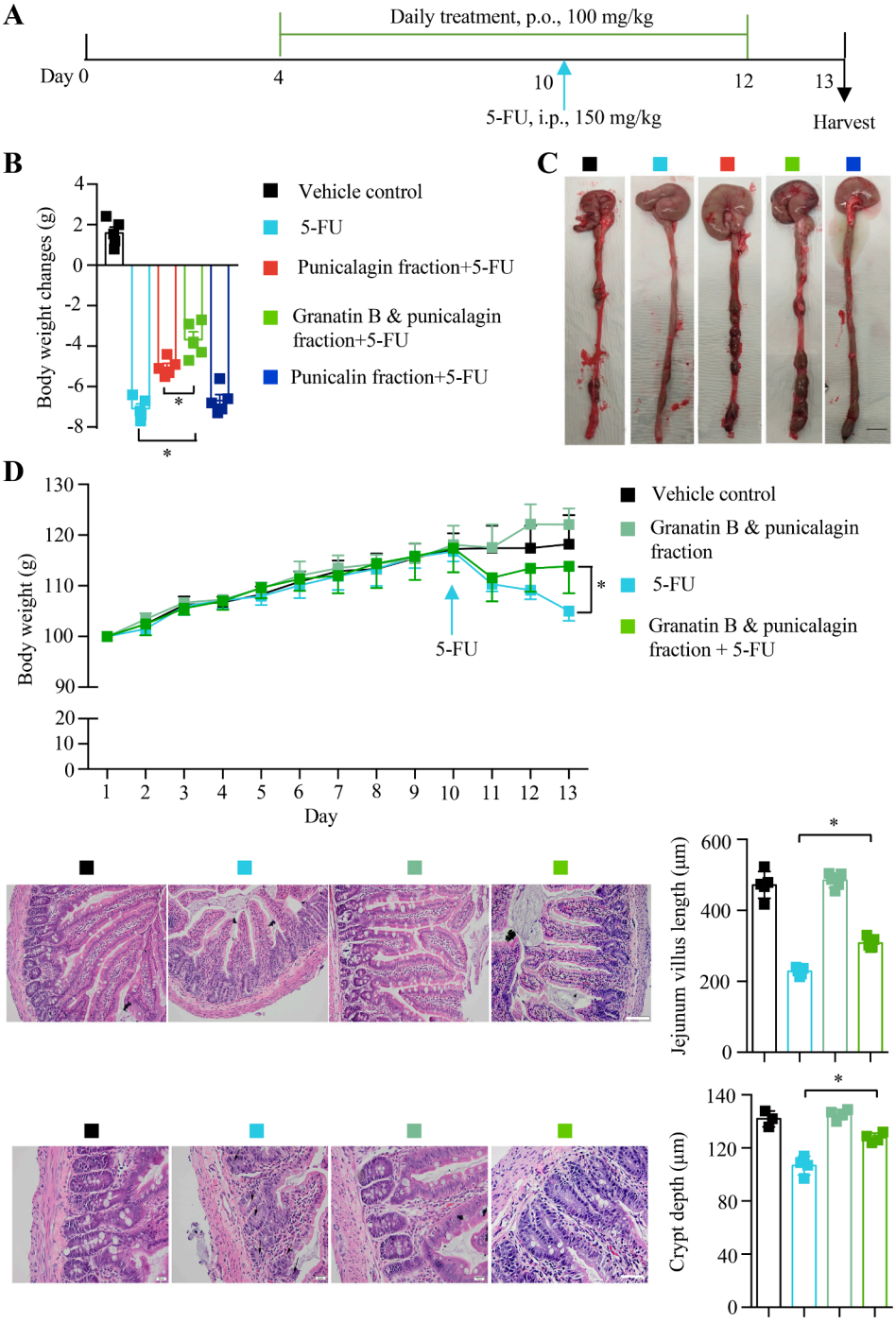

Fig. 8. Effects of the ellagitannins on 5-FU-induced intestinal mucositis. (**A**) Experimental scheme. (**B**) Body weight variation three days after 5-FU treatment. (**C**) Macroscopic images of colons and stool. (**D**) Body weight changes and histological images of the jejunum and quantitative results. Scale bars: 50 μm. Values reported as mean ± SD. B, $n = 5$, D, $n = 3$–8. *$p < 0.05$.

the same order as experiments above: granatin B and punicalagin, punicalagin, and then punicalin (Fig. 7B). The effects of granatin B and punicalagin on LPS-induced IL-6 production, iNOS production, and NF-κB p65 nuclear translocation were further investigated. IL-6 and iNOS productions were dose-dependently inhibited by granatin B and punicalagin (Fig. 7C). Moreover, granatin B and punicalagin blocked LPS-induced p65 nuclear import considerably while having no effect on p65 expression (Fig. 7C,D). Collectively, the results show granatin B and punicalagin can ameliorate LPS-induced ROS, No., IL-6, and iNOS production in RAW264.7 cells, possibly by inhibiting NF-κB signaling.

Effects of granatin B and punicalagin on intestinal mucositis

Anti-mucositis activities of the ellagitannins were investigated in 5-FU-treated rats (Fig. 8A). Exposure of the animals to a single dose of 5-FU severely affected their health conditions; dramatic body weight loss and diarrhea lasting more than three days was observed. Granatin B and punicalagin fraction most significantly ameliorated 5-FU-induced loss of body weight and watery stool among the three fractions tested (Fig. 8B,C). Particularly, after granatin B and punicalagin treatment, the color of the stool turned black and the texture became harder compared to the pale and soft texture of the stool in the 5-FU-treated group. Moreover, stool of the control group as well as the granatin B and punicalagin group formed solid pellets in the colon segment while stool of the 5-FU-treated group did not (Fig. 8C). Therefore, the effects of granatin B and punicalagin on intestinal mucositis were further explored. Granatin B and punicalagin treatment did not significantly alter body weight. After 5-FU treatment on day 10, the body weight of the rats decreased time-dependently with the most significant reduction observed on day 13. On this day, when treated together with 5-FU, granatin B and punicalagin attenuated the significant body weight loss observed in the group treated only with 5-FU (Fig. 8D). Histology analysis showed that granatin B and punicalagin ameliorated 5-FU-induced villus shortening and crypt depth reduction without inducing any pathological changes in vital organs (Figs. 8D and S18). In summary, the results indicate that granatin B and punicalagin exhibit potent anti-5-FU-induced mucositis activities.

Discussion

Colorectal cancer is one of the most common cancers affecting millions of people today. Current 5-FU-based first-line chemotherapy for colorectal cancer often leads to chemoresistance. Development of adverse effects, such as mucositis, is also inevitable. Therefore, this study aimed to find potential therapeutic agents with anti-colorectal cancer and anti-mucositis activities in Chinese herbal medicine. It was revealed that the major targets of compounds in pomegranate peels were colorectal cancer and inflammatory diseases. However, the numerous compounds in pomegranate peels posed a challenge for further exploration of the roles of active individual compounds and their mechanisms in biological systems. *In vitro* antioxidant activities of bioactive chemicals generally are good proxies for their bioactivities (Wang et al., 2016). In this study, antioxidant activity-guided investigation of pomegranate peel extracts identified punicalagin and granatin B as potent antioxidant compounds. In support of this, punicalagin has been reported to possess strong DPPH• and superoxide radicals scavenging activities as well as lipid peroxidation inhibitory activities in a liposome model system (Kulkarni et al., 2004). Punicalagin showed scavenging activities against multiple one-electron oxidizing radicals, including •OH, N3•, and NO2• (Kulkarni et al., 2007). Another study reports that among four ellagitannins purified from pomegranate peels – granatin B, punicalagin, punicalin, and strictinin A – granatin B showed the strongest inhibitory effects against iNOS and COX-2 (Lee et al., 2010). Our results further complement this study and suggest that granatin B possesses much stronger antioxidant activity than that of punicalagin.

We then explored the anti-colorectal cancer and -inflammatory activities of granatin B and punicalagin. The granatin B and punicalagin fraction exhibited both superior anti-colorectal cancer and -inflammatory activities compared to the punicalagin or punicalin fractions. The granatin B and punicalagin fraction induced both dose- and time-dependent cytotoxicity in HT-29 cells while it significantly attenuated LPS-induced generation of NO, iNOS, ROS, IL-6, and blocked the nuclear localization of NF-κB p65 in RAW 264.7 cells. To confirm these *in vitro* activities, anti-HT-29 cell and anti-intestinal mucositis activities were further investigated in HT-29 xenograft tumor models and 5-FU-treated rats, respectively. Consistent with the *in vitro* results, *in vivo* results showed that the granatin B and punicalagin fraction exhibited the strongest anti-HT-29 xenograft tumor and anti-mucositis activities. Granatin B has been reported to inhibit proliferation of glioma and lung cancer cells *in vitro* (Jin et al., 2016; Toda et al., 2020). However, the *in vivo* effects of granatin B on cancer cells have not been established. Simultaneous targeting of colorectal cancer cells and mucositis by granatin B and punicalagin makes them an attractive anti-colorectal cancer agent. Therefore, it would be interesting to compare the anti-colorectal cancer and anti-mucositis activities of the punicalagin and granatin B compounds individually in future studies.

Cell death mechanisms of granatin B and punicalagin on HT-29 cells were further examined. Our results indicate that granatin B and punicalagin induced apoptosis through both cell death receptor- and mitochondria-mediated pathways. In most advanced tumors, cancer cells exhibit alteration of apoptotic pathways and develop drug resistance against chemotherapeutic agents (Molinari, 2000). Therefore, inducing apoptosis in cancer cells is an important strategy against carcinogenesis. Moreover, arresting cell cycle activity is another effective anti-cancer strategy as cell cycle regulators are frequently dysregulated in various cancers, including colorectal cancer (Cancer Genome Atlas, 2012). Granatin B and punicalagin arrested the cells in S-phase. Thus, granatin B and punicalagin appear to be a promising therapeutic agent against colorectal cancer. Furthermore, it has been reported that ROS stress-induced DNA damage and protein modification may result in cellular dysfunction such as cell cycle arrest and apoptosis (Jackson and Bartek, 2009; Shi et al., 2014). In our study, granatin B and punicalagin increased ROS production in a dose-dependent manner. Additionally, mitochondrial protein SOD 2 but not cytoplasmic protein SOD 1 was downregulated, indicating the involvement of the mitochondria in granatin B and punicalagin-induced ROS stress. Furthermore, the antioxidant NAC is known to inhibit ROS-dependent apoptosis (Curtin et al., 2002). Likewise, NAC ameliorated granatin B and punicalagin-induced ROS stress, apoptosis, and cell cycle arrest. Granatin B and punicalagin toxicity against HT-29 cells was also attenuated by NAC pretreatment. Collectively, our results suggest that granatin B and punicalagin induces ROS-mediated cell cycle arrest and apoptosis in HT-29 cells.

Our study is novel in that the cytotoxicity and cell death mechanism of granatin B against HT-29 colorectal cancer cells, ROS-mediated apoptosis and cell cycle arrest of colorectal cancer cells caused by punicalagin, and the *in vivo* efficacy of both granatin B and punicalagin in colorectal cancer treatment have not been previously explored. Polyphenols have been reported to generate oxidative stress specifically in cancer cells via intracellular copper mobilization since copper concentrations are significantly elevated in cancer cells (Khan et al., 2014). Therefore, granatin B and punicalagin might become pro-oxidant in HT-29 colorectal cancer cells and induce oxidative stress-mediated cell death through intracellular copper mobilization. In future studies, we plan on comparing the concentration of copper ions in HT-29 colorectal cancer cells with non-cancerous cell lines or primary cells.

Granatin B and punicalagin also enhanced 5-FU-induced cell death and cell cycle arrest in HT-29 cells. 5-FU-induced autophagy in HT-29 cells has been reported to be a mechanism of colorectal cancer resistance to 5-FU (Sui et al., 2014); this was consistent in our study. In contrast, granatin B and punicalagin inhibited autophagy in HT-29 cells. Therefore, inhibition of autophagy may contribute to the enhanced cytotoxicity of 5-FU when administered together with granatin B and

punicalagin in HT-29 cells. Additionally, granatin B and punicalagin inhibited p65 nuclear import in HT-29 cells, which has been shown to suppress cell proliferation and the cell cycle, while in turn inducing apoptosis (Zhang et al., 2017b). The inhibition of NF-κB p65 nuclear import may contribute to the enhanced cell death caused by the combined treatment and could be the link for granatin B and punicalagin's anti-HT-29 cell and anti-LPS-induced inflammatory activities in RAW 264.7 cells.

Conclusion

Granatin B and punicalagin exhibit strong anti-colorectal cancer and anti-mucositis activities. Granatin B and punicalagin induced HT-29 cell death via ROS-mediated cell cycle arrest and apoptosis induction, and further sensitized HT-29 colorectal cancer cells to 5-FU-induced cell death. Collectively, our results provide evidence for developing granatin B and punicalagin as a potential therapeutic agent for colorectal cancer and mucositis. With this, we hope to highlight the possibility of utilizing phenols from herbal medicine as a potential strategy for treatment of colorectal and other cancers.

CRediT authorship contribution statement

Xiao-Xin Chen: Visualization, Formal analysis, Data curation, Writing – original draft. **Sheamin Khyeam:** Formal analysis, Data curation, Writing – original draft. **Zhang-Jin Zhang:** Visualization, Writing – original draft. **Kalin Yan-Bo Zhang:** Visualization, Writing – original draft.

Declaration of Competing Interest

None.

Acknowledgments

This work is supported by Innovation and Technology Support Programme, Government of Hong Kong (Project code: UIM/321, to Z.K.Y. B.), Seed Fund for Basic Research from University of Hong Kong (Project code: 201611159232, to Z.K.Y.B), American Heart Association Postdoctoral Fellowship (Project code: 828442, to C.X.X.). The founders were not involved in the design, analysis or writing of this article.

Supplementary materials

Supplementary material associated with this article can be found, in the online version, at doi:10.1016/j.phymed.2022.153923.

References

Ahluwalia, A., K Jones, M., Matysiak-Budnik, T., S Tarnawski, A., 2014. VEGF and colon cancer growth beyond angiogenesis: does VEGF directly mediate colon cancer growth via a non-angiogenic mechanism? Curr. Pharm. Des. 20, 1041–1044.

Cancer Genome Atlas, N., 2012. Comprehensive molecular characterization of human colon and rectal cancer. Nature 487, 330–337.

Chen, X., Lam, K., Feng, Y., Xu, K., Sze, S., Tang, C., Leung, G., Lee, C., Shi, J., Yang, Z., 2018. Ellagitannins from pomegranate ameliorates 5-fluorouracil-induced intestinal mucositis in rats while enhancing its chemotoxicity against HT-29 colorectal cancer cells through intrinsic apoptosis induction. J. Agric. Food Chem. 66, 7054–7064.

Chen, X.X., Feng, H.L., Ding, Y.M., Chai, W.M., Xiang, Z.H., Shi, Y., Chen, Q.X., 2014. Structure characterization of proanthocyanidins from *Caryota ochlandra* hance and their bioactivities. Food Chem. 155, 1–8.

Chen, X.X., Lam, K.H., Chen, Q.X., Leung, G.P., Tang, S.C.W., Sze, S.C., Xiao, J.B., Feng, F., Wang, Y., Zhang, K.Y., et al., 2017a. *Ficus virens* proanthocyanidins induced apoptosis in breast cancer cells concomitantly ameliorated 5-fluorouracil induced intestinal mucositis in rats. Food Chem. Toxicol. 110, 49–61.

Chen, X.X., Leung, G.P.H., Zhang, Z.J., Xiao, J.B., Lao, L.X., Feng, F., Mak, J.C.W., Wang, Y., Sze, S.C.W., Zhang, K.Y.B., 2017b. Proanthocyanidins from *Uncaria rhynchophylla* induced apoptosis in MDA-MB-231 breast cancer cells while enhancing cytotoxic effects of 5-fluorouracil. Food Chem. Toxicol. 107, 248–260.

China Pharmacopea Committee, 2010. The People's Republic of China Pharmacopoeia. Chinese medicine science and Technology Press, Beijing, China.

Curtin, J.F., Donovan, M., Cotter, T.G., 2002. Regulation and measurement of oxidative stress in apoptosis. J. Immunol. Methods 265, 49–72.

Fischer, U.A., Carle, R., Kammerer, D.R., 2011. Identification and quantification of phenolic compounds from pomegranate (*Punica granatum* L.) peel, mesocarp, aril and differently produced juices by HPLC-DAD-ESI/MS(n). Food Chem. 127, 807–821.

Garcia-Villalba, R., Espin, J.C., Aaby, K., Alasalvar, C., Heinonen, M., Jacobs, G., Voorspoels, S., Koivumaki, T., Kroon, P.A., Pelvan, E., 2015. Validated method for the characterization and quantification of extractable and nonextractable ellagitannins after acid hydrolysis in pomegranate fruits, juices, and extracts. J. Agric. Food Chem. 63, 6555–6566.

Jackson, S.P., Bartek, J., 2009. The DNA-damage response in human biology and disease. Nature 461, 1071–1078.

Jin, Z., Yu, Y., Jin, R.H., Wang, Y.B., Xu, H.Y., 2016. Effect of granatin B on the glioma cancer by inducing apoptosis. Am. J. Transl. Res. 15, 3970–3975.

Khan, H.Y., Zubair, H., Faisal, M., Ullah, M.F., Farhan, M., Sarkar, F.H., Ahmad, A., Hadi, S.M., 2014. Plant polyphenol induced cell death in human cancer cells involves mobilization of intracellular copper ions and reactive oxygen species generation: a mechanism for cancer chemopreventive action. Mol. Nutr. Food Res. 58, 437–446.

Kilkenny, C., Browne, W., Cuthill, I.C., Emerson, M., Altman, D.G., 2010. Animal research: reporting *in vivo* experiments: the ARRIVE guidelines. Br. J. Pharmacol. 160, 1577–1579.

Kulkarni, A.P., Aradhya, S.M., Divakar, S., 2004. Isolation and identification of a radical scavenging antioxidant-punicalagin from pith and carpellary membrane of pomegranate fruit. Food Chem. 87, 551–557.

Kulkarni, A.P., Mahal, H.S., Kapoor, S., Aradhya, S.M., 2007. *In vitro* studies on the binding, antioxidant, and cytotoxic actions of punicalagin. J. Agric. Food Chem. 55, 1491–1500.

Lee, C.J., Chen, L.G., Liang, W.L., Wang, C.C., 2010. Anti-inflammatory effects of *Punica granatum* Linne *in vitro* and *in vivo*. Food Chem. 118, 315–322.

Mohammad, S.M., Kashani, H.H., 2012. Chemical composition of the plant *Punica granatum* L.(Pomegranate) and its effect on heart and cancer. J. Med. Plants Res. 6, 5306–5310.

Molinari, M., 2000. Cell cycle checkpoints and their inactivation in human cancer. Cell Prolif. 33, 261–274.

Oszmianski, J., Wojdylo, A., Lamer-Zarawska, E., Swiader, K., 2007. Antioxidant tannins from rosaceae plant roots. Food Chem. 100, 579–583.

Ouyang, L., Shi, Z., Zhao, S., Wang, F.T., Zhou, T.T., Liu, B., Bao, J.K., 2012. Programmed cell death pathways in cancer: a review of apoptosis, autophagy and programmed necrosis. Cell Prolif. 45, 487–498.

Poyrazoglu, E., Gokmen, V., Artik, N., 2002. Organic acids and phenolic compounds in pomegranates (*Punica granatum* L.) grown in Turkey. J. Food Compos. Anal. 15, 567–575.

Price, A.E., Shamardani, K., Lugo, K.A., Deguine, J., Roberts, A.W., Lee, B.L., Barton, G. M., 2018. A map of toll-like receptor expression in the intestinal epithelium reveals distinct spatial, cell type-specific, and temporal patterns. Immunity 49, 560–575 e566.

Schumacker, P.T., 2006. Reactive oxygen species in cancer cells: live by the sword, die by the sword. Cancer Cell 10, 175–176.

Shi, Y., Nikulenkov, F., Zawacka-Pankau, J., Li, H., Gabdoulline, R., Xu, J., Eriksson, S., Hedström, E., Issaeva, N., Kel, A., 2014. ROS-dependent activation of JNK converts p53 into an efficient inhibitor of oncogenes leading to robust apoptosis. Cell Death Differ. 21, 612–623.

Sui, X.B., Kong, N., Wang, X., Fang, Y., Hu, X.T., Xu, Y.H., Chen, W., Wang, K.F., Li, D., Jin, W., 2014. JNK confers 5-fluorouracil resistance in p53-deficient and mutant p53-expressing colon cancer cells by inducing survival autophagy. Sci. Rep. 4, 4694. Uk.

Sun, L.Q., Ding, X.P., Qi, J., Yu, H., He, S.A., Zhang, J., Ge, H.X., Yu, B.Y., 2012. Antioxidant anthocyanins screening through spectrum-effect relationships and DPPH-HPLC-DAD analysis on nine cultivars of introduced rabbiteye blueberry in China. Food Chem. 132, 759–765.

Toda, K., Ueyama, M., Tanaka, S., Tsukayama, I., Mega, T., Konoike, Y., Tamenobu, A., Bastian, F., Akai, I., Ito, H., Kawakami, Y., Takahashi, Y., Suzuki-Yamamoto, T., 2020. Ellagitannins from *Punica granatum* leaves suppress microsomal prostaglandin E synthase-1 expression and induce lung cancer cells to undergo apoptosis. Biosci. Biotechnol. Biochem. 84, 757–763.

Wang, J.Q., Hu, S.Z., Nie, S.P., Yu, Q., Xie, M.Y., 2016. Reviews on mechanisms of *in vitro* antioxidant activity of polysaccharides. Oxidative Med. Cell. Longev. 2016, 5692852.

Wang, H., Liu, Y., Ding, J., Huang, Y., Liu, J., Liu, N., Ao, Y., Hong, Y., Wang, L., Zhang, L., 2020. Targeting mTOR suppressed colon cancer growth through 4EBP1/eIF4E/PUMA pathway. Cancer Gene Ther. 27, 448–460.

Wild, C.P., Weiderpass, E., Stewart, B.W., 2020. World Cancer Report: Cancer Research For Cancer Prevention. International Agency for Research on Cancer, Lyon, France.

Zhang, L.N., Song, R.L., Gu, D.S., Zhang, X.L., Yu, B.Q., Liu, B.Y., Xie, J.W., 2017a. The role of GLI1 for 5-FU resistance in colorectal cancer. Cell Biosci. 7, 17.

Zhang, Q., Lenardo, M.J., Baltimore, D., 2017b. 30 Years of NF-kappa B: a blossoming of relevance to human pathobiology. Cell 168, 37–57.

Zhang, Y., Zhang, L.H., Liu, J.J., Liang, J.L., Si, J.P., Wu, S.H., 2017c. *Dendrobium officinale* leaves as a new antioxidant source. J. Funct. Foods 37, 400–415.